Copolymer Morphologies

DOI: 10.1002/anie.200802834

Cryo Electron Tomography Reveals Confined Complex Morphologies of Tripeptide-Containing Amphiphilic Double-Comb Diblock Copolymers**

Alison L. Parry, Paul H. H. Bomans, Simon J. Holder, Nico A. J. M. Sommerdijk,* and Stefano C. G. Biagini**

The property of amphiphilic block copolymers to form self-assembled structures in aqueous media has been known and studied for many years.[1] This form of self-assembly is known to produce a wide range of morphologies, the most common being spherical micelles, cylindrical micelles, and vesicles.[1] Over the past decade a number of other morphologies have been observed, including stacked micelles,[2] toroids,[3] hexagonally packed hoola hoops,[4] helices,[5] and branched structures.[6] Initially linear diblock copolymers were the main type of macromolecules used for these studies; however, in later investigations the toolbox of polymer self-assembly was extended to the use of dendrimers[7] and branched[8] polymer segments as one of the blocks, but also ABA,[9] ABC,[10] and multiblock[11] copolymers have been explored.

A separate class of amphiphiles is formed by comblike block polymers. These have one or more segments composed of a central polymer backbone with polymeric or oligomeric side chains. Comblike polymers exist with hydrophobic[12] as well as hydrophilic side chains[13] and also as random copolymers with both types of side chains.[14] Recently some of us used the same strategy for the synthesis of norbornene-based double-comb diblock polymers containing oligo(ethylene oxide) (OEG) side chains in one block and a specific peptide sequence in the other block.[15]

Herein we report how this new polymer architecture (see also the Supporting Information) allows us to modify the self-assembly behavior specifically through the introduction of different amino acids in the hydrophobic block. Moreover, we show how the complex morphologies resulting from the aggregation of these amphiphilic double-comb diblock copolymers can be analyzed and visualized in nanometer detail by using cryo electron tomography (cryoET).

[*] Dr. A. L. Parry, Dr. S. J. Holder, Dr. S. C. G. Biagini
Functional Materials Group, Chemical Laboratory, School of Physical Sciences, University of Kent at Canterbury
Canterbury, Kent, CT2 7NR (UK)
Fax: (+44) 1227-827-558
E-mail: s.c.g.biagini@kent.ac.uk
s.j.holder@kent.ac.uk

P. H. H. Bomans, Dr. N. A. J. M. Sommerdijk
Laboratory of Materials and Interface Chemistry and Soft Matter Cryo-TEM Research Unit, Eindhoven University of Technology
PO Box 513, 5600 MB, Eindhoven (The Netherlands)
E-mail: n.sommerdijk@tue.nl

[**] We thank Dr. K. Lyakhova for valuable discussions.

Supporting information for this article is available on the WWW under http://dx.doi.org/10.1002/anie.200802834.

Dynamic light scattering (DLS) analysis of 1 wt% dispersions of the block copolymer indicated the formation of stable aggregates with diameters of 50–450 nm for PNOEG–PNGLF (**1**) and 80–280 nm for PNOEG–PNLVL (**2**) (see

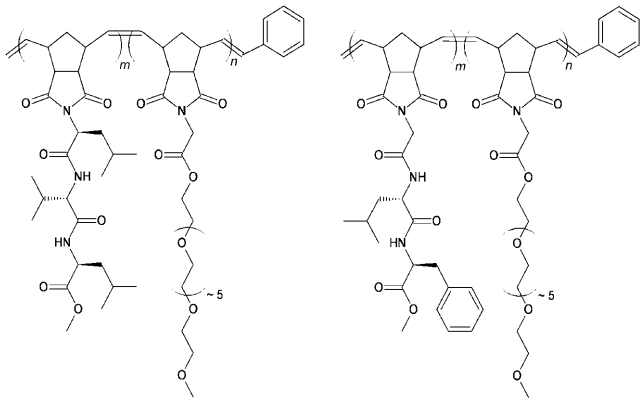

1 PNOEG-PNGLF, *m*=50, *n*=50
2 PNOEG-PNLVL, *m*=50, *n*=50
3 PNOEG, *m*=0, *n*=50
4 PNGLF, *m*=50, *n*=0
5 PNLVL, *m*=50, *n*=0
6 PNOEG-PNGGG, *m*=50, *n*=50
7 PNOEG-PNGL, *m*=0, *n*=50

Figure SI1 in the Supporting Information). The morphology of these aggregates was investigated with conventional (negative staining) as well as cryogenic (cryo) TEM, both of which showed that the two block copolymers both formed unprecedented, complex morphologies (Figures 1 and 2). GLF-based block copolymer **1** was observed to form large spherical aggregates that showed internal microphase separation (Figure 1a,b). The LVL-derived block copolymer (**2**) also displayed an unusual aggregate morphology, which appeared to consist of tightly coiled wormlike micelles (Figure 2a,b).

CryoTEM has now been established as an important technique for the 2D visualization of a large range of self-assembled structures in solution.[16] CryoET involves the acquisition of a series of cryoTEM images under different tilt angles and the subsequent computer-assisted reconstruction of the original 3D volume. Although cryoET has been recognized as a strong and emerging technique in the biological sciences,[17] it is still virtually unexplored for the analysis of samples of synthetic origin.[18]

To elucidate the structure of the aggregates of **1** and **2** completely, vitrified samples were studied by low-dose

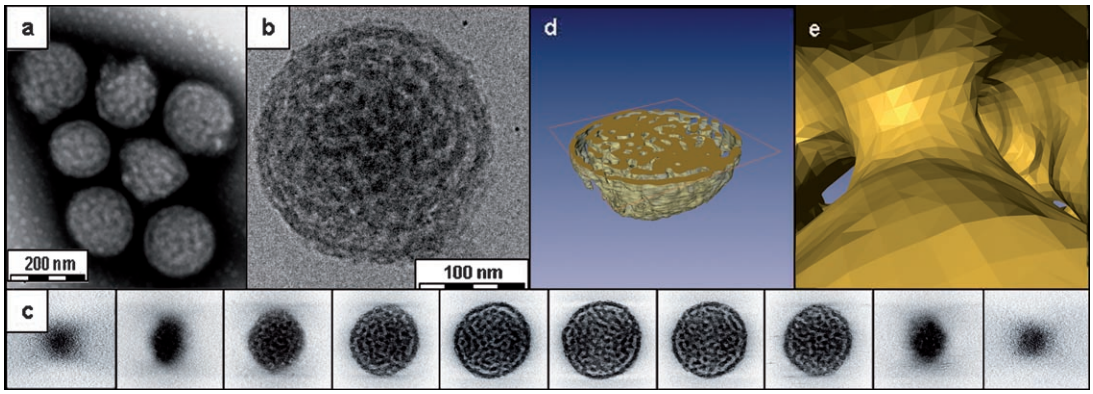

Figure 1. TEM analysis of aggregates of PNOEG–PNGLF (**1**). a) Conventional TEM using negative staining; b) cryoTEM image of a vitrified film; c) gallery of *z* slices showing different cross sections of a 3D SIRT (simultaneous iterative reconstruction technique) reconstruction of a tomographic series recorded from the vitrified film in (b); d,e) visualization of the segmented volume showing d) a cross section of the aggregate and e) a view from within the hydrated channels.

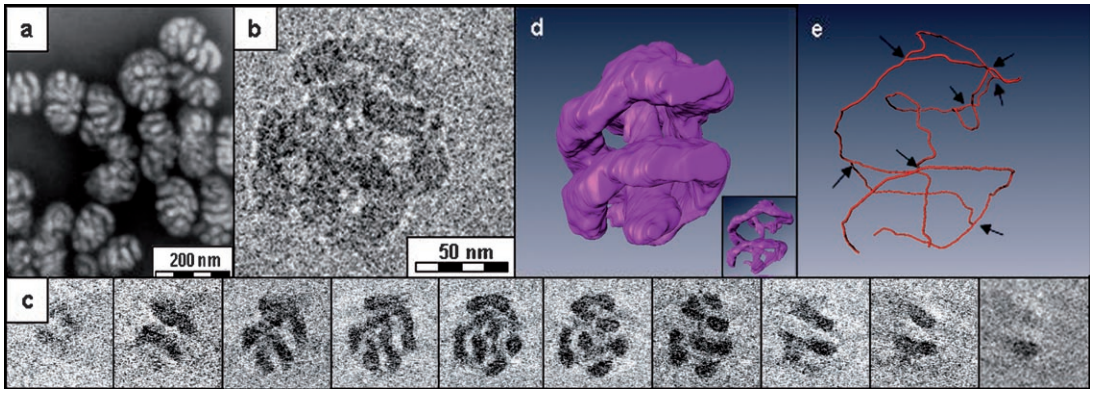

Figure 2. TEM analysis of aggregates of PNOEG–PNLVL (**2**). a) Conventional TEM using negative staining; b) cryoTEM image of a vitrified film; c) gallery of *z* slices showing different cross sections of a 3D volume reconstructed from a tomographic series recorded from the vitrified film in (b); d) visualization of the segmented volume before and after (inset) artificial thinning; e) skeletonization of the aggregate structure highlighting the branching points (arrows) and loops in the aggregate.

cryoET. Analysis of the reconstructed 3D volume shows that the assemblies of **1** consist of a spherical aggregate, the interior of which is formed by an interpenetrating network of dark, electron-opaque, and lighter, almost electron-transparent regions, forming a bicontinuous assembly in which the branched network of wormlike hydrophobic peptide-containing segments are segregated from channels containing the hydrated OEG moieties. Detailed analysis of the individual slices (Figure 1c) from the reconstructed volume revealed that the hydrophobic domains have an average cross section of 20 ± 2 nm, whereas the average cross section of the water channels is 15 ± 2 nm. The *z* slices of the reconstruction further showed that the apparent shell that encloses the bicontinuous network inside the aggregates has perforations connecting the internal and external aqueous phases. Segmentation was used to generate graphical representations that clearly demonstrated the 3D structure of these aggregates, highlighting both the bicontinuous structure and the perforations in the encapsulating shell (Figure 1d,e).

Inspection of the reconstructed volume of the aggregates of **2** revealed that the coiled globular aggregates consist of single wormlike micelles with diameters of 20 ± 2 nm. Moreover, the aggregate is folded such that linear micellar segments are placed at the same average distance of around 20–25 nm from each other within the aggregate. Again segmentation was used to illustrate the morphological features that are not evident from the *x*–*y* cross sections of the 3D volume (Figure 2c) The resulting 3D visualization of the volume of the aggregate (Figure 2d) was further reduced by thinning (inset) and skeletonization (Figure 2e) to show that these wormlike structures contain several branches and loops within a single aggregate.

To investigate the role of the different macromolecular components in the self-assembly of the block copolymers, we also investigated with conventional TEM the aggregation behavior of the different polymer blocks (**3**–**5**) alone as well as that of block copolymers **6** and **7**. Upon dispersion of the OEG-derived homopolymer (**3**) in water, poorly defined aggregates were formed (see Figure SI2 in the Supporting Information). In contrast, OEG-grafted polymethacrylate can be molecularly dissolved in water, which argues for a role of the poly(norbornene) (PN) backbone in contributing to the hydrophobic domains of the aggregates.[19] Surprisingly, for the peptide-based homopolymers **4** and **5**, conventional TEM indicated the formation of vesicular aggregates (see Figure SI2), even though they consist largely of water-insoluble

material. However, these aggregates had limited stability and rapidly precipitated, after which they could not be redispersed, suggesting that the hydrophobic PN–peptide block is able to undergo conformational rearrangement in aqueous medium. This result also implies that the aggregates of **1** and **2** are not simply kinetically trapped states, formed as a consequence of the addition of water, but that the hydrophobic domains are able to adapt their shape and organization to minimize the surface energy during the aggregation process.

^{1}H NMR spectra from the aggregates of **1** and **2** were obtained by freeze-drying the aqueous dispersions and redispersing them in D_2O. The only signals visible in the spectra for **1** and **2** were those of the OEG component. (see Figures SI3 and SI4 in the Supporting Information). The absence of any signals for the PN backbone or peptide side chains suggests that these components are aggregated. ^{1}H NMR relaxation times are influenced by changes in the dynamic motion of protons. T_2 relaxation times decrease as molecular motion decreases and in quasi-glassy cores the signals are broadened beyond detection by NMR spectroscopy.[20,21] The implication that the hydrophobic regions of the aggregates are formed by not only the peptide side chain but also by the entire PN backbone was supported by the finding that also for micellar dispersions of the OEG-derived homopolymer **3** no signals for the PN backbone were visible in the ^{1}H NMR spectra.

The above observations suggest the back folding of the OEG-modified PN backbone onto the peptide-modified PN part, together forming the hydrophobic domains in the aggregates observed in cryoTEM. This result underlines that block copolymers **1** and **2** cannot be considered as simple AB diblock amphiphilic copolymers. It is important to note that the length of the OEG chains (ca. 7 units; extended length of 2.0–2.5 nm) is far less than what is required to fill the hydrophilic domains within the boundaries of the aggregates (approximate dimensions 15 nm for **1** and 20–25 nm for **2**) and that this component will merely form a thin, hydrated layer separating the approximately 20 nm thick hydrophobic domains from the water.

As both polymers had the same weight fraction of OEG grafts ($W_{OEG} = 0.33$, see the Supporting Information) and comparable molecular weights, we attribute the difference in aggregation behavior to the specific amino acid sequence of the peptide graft. In support of this statement, we investigated the aggregation behavior of two related polymers PNOEG–PNGGG (**6**) and PNOEG–PNGL (**7**), which both have the same molecular weight (45 kg mol^{-1}) and similar W_{OEG} values (0.38 for **6** and 0.39 for **7**) but differ distinctly in their aggregation behavior (see the Supporting Information). Conventional TEM (Figure SI2 in the Supporting Information) showed that PNOEG–PNGGG (**6**) formed small clustered micelles, a number of which showed a tendency to elongate, whereas PNOEG–PNGL (**7**) surprisingly formed the same spherical aggregates with an internal network structure as were observed for **1** (Figure 1). The latter observation suggests that the presence of the glycine–leucine sequence, rather than the precise value of W_{OEG} is critical in the formation of the aggregates observed for **1**.

The effect of molecular weight, polydispersity (PDI), and polymer composition on the aggregation behavior of amphiphilic diblock copolymers has been carefully documented.[6,22,23] In general, a decrease in the weight fraction of the hydrophilic segment(s) leads to a decrease of the spontaneous curvature of the aggregates going from spherical micelles to cylindrical micelles and eventually bilayer aggregates. For polymers with moderate spontaneous curvature, it has been demonstrated that also branched structures and highly curved structures can be formed. Although the energy of these aggregates is optimized when these cylinders have uniform curvature, for example, in the form of straight rodlike structures, system entropy can introduce bending as well as branching of the cylinders. We can consider the aggregates of **1** and **2** as two different types of cylindrical structures with varying degrees of branching.

The branching of cylindrical micelles, that is, both the formation of networks and individual Y junctions, is associated with defect formation and has been attributed to a frustrated packing of the polymer segments inside the aggregate. Polymer aggregates have been shown not to exchange monomers because of the extremely low critical micelle concentration (CMC) of polymer amphiphiles. Consequently, for non-monodisperse polymers such as **1** and **2** (PDI 2.7 and 1.9, respectively; see the Supporting Information), the aggregates have to accommodate macromolecules with quite different spontaneous curvature. Bates and Jain demonstrated that local segregation of polymer chains with the similar length and composition can lead to the formation of regions and segments with different curvature.[22b] We propose that in the present case the polydispersity of **1** and **2** accommodates the formation of branches, folds, and loops. More precisely, for **1** the formation of many Y junctions gives rise to a highly branched, bicontinuous network, whereas for the aggregates of **2** the surface energy is optimized predominantly by the high curvature of the cylinders, and only to a lower extent by the formation of Y junctions.

To our knowledge the aggregates observed for **1** and **2** are unique and unprecedented structures. One remarkable aspect of the aggregates of **1** is that the network structure does not extend into solution but seems to be confined within a perforated shell.[23] Similarly, the wormlike structures formed by **2** are extensively folded such that globular architectures are formed (Figure 2a). Although such structures have not yet been observed experimentally, both have been described as the results from the molecular modeling studies of amphiphilic diblock copolymers in which droplets of the polymer were dropped into a water bath, after which a phase separation developed inside the confinement of the droplet.[24,25] Under the experimental conditions used, it is conceivable that the dropwise addition of water to a solution of the polymers in DMSO causes a phase separation, leading to the formation of DMSO–polymer droplets in an aqueous volume. Following from such a situation, one may speculate that the subsequent exchange of DMSO with water induces the microphase separation that eventually results in the polymer structures observed.

Importantly, in the above-mentioned simulation of Fraaije and Sevinck, the different structures (folded worms, inter-

penetrating networks) arise as a function of the block length ratios,[24] whereas in the present case these are the result of different peptide sequences in the side chains. However, for a given block copolymer system, the different structures in the phase diagrams can also be obtained by adjusting the different interaction parameters (χ), which is highly likely to occur upon changing the amino acid sequence in the side chains going from **1** to **2.**

In conclusion, we have investigated a new type of double-comb diblock copolymer, in which one comb of polymer blocks contains hydrophilic OEG side chains and the other contains more hydrophobic tripeptide side chains. Upon dispersion in water, these form unprecedented aggregates that were analyzed in detail by cryoET. The power of this technique enabled us to establish that the 3D structure of the aggregates was characterized by a high degree of branching and extreme curvature of the essentially micellar assemblies. We demonstrated that the type of aggregates formed was directed by the specific peptide sequence rather than by the hydrophilic–hydrophobic balance of the polymers used, although no evidence was obtained for a specific structural organization of the peptide chains inside the polymer aggregates. One intriguing and not fully resolved aspect remains that the aggregate structures seem to exist within the apparent spherical boundaries of the droplets that may have formed upon the addition of water to the original polymer–solvent solution. It is reasonable to assume that the relatively broad molecular weight distributions (PDI = 1.9–2.7) of the polymers facilitates the formation of such complex morphologies in a single aggregate structure by phase separation into domains with different preferred curvature.

Experimental Section

See the Supporting Information.

Received: June 15, 2008
Published online: September 11, 2008

Keywords: aggregation · branching · electron microscopy · polynorbornene · self-assembly

[1] a) D. E. Discher, A. Eisenberg, *Science* **2002**, *297*, 967–973; b) M. Antonietti, S. Förster, *Adv. Mater.* **2003**, *15*, 1323–1333.
[2] Z. Li, E. Kesselman, Y. Talmon, M. A. Hillmyer, T. P. Lodge, *Science* **2004**, *306*, 98–101.
[3] D. J. Pochan, Z. Chen, H. Cui, . K. Hales, K. Qi, K. L. Wooley, *Science* **2004**, *306*, 94–97.
[4] L. Zhang, C. Bartels, Y. Yu, H. Shen, A. Eisenberg, *Phys. Rev. Lett.* **1997**, *79*, 5034–5037.
[5] J. J. L. M. Cornelissen, M. Fischer, N. A. J. M. Sommerdijk, R. J. M. Nolte, *Science* **1998**, *280*, 1427–1430.
[6] S. Jain, F. S. Bates, *Science* **2003**, *300*, 460–464.
[7] a) J. C. M. van Hest, D. A. P. Delnoye, M. W. P. L. Baars, M. H. P. van Genderen, E. W. Meijer, *Science* **1995**, *268*, 1592; b) I. Gitsov, J. M. J. Fréchet, *J. Am. Chem. Soc.* **1996**, *118*, 3785–3786.
[8] a) R. Matmour, R. Francis, R. S. Duran, Y. Gnanou, *Macromolecules* **2005**, *38*, 7754–7767; b) A. Heise, J. L. Hedrick, C. W. Frank, R. D. Miller, *J. Am. Chem. Soc.* **1999**, *121*, 8647–8648.
[9] a) J. Grumelard, A. Taubert, W. Meier, *Chem. Commun.* **2004**, 1462–1463; b) N. Chebotareva, P. H. H. Bomans, P. M. Frederik, N. A. J. M. Sommerdijk, R. P. Sijbesma, *Chem. Commun.* **2005**, 4967–4969.
[10] Z. Li, E. Kesselman, Y. Talmon, M. A. Hillmyer, T. P. Lodge, *Science* **2004**, *306*, 98–101; H. Cui, Z. Chen, S. Zhong, K. L. Wooley, D. J. Pochan, *Science* **2007**, *317*, 647–650.
[11] a) S. J. Holder, R. C. Hiorns, N. A. J. M. Sommerdijk, R. G. Jones, R. J. M. Nolte, *Chem. Commun.* **1998**, 1445; b) N. A. J. M. Sommerdijk, S. J. Holder, R. C. Hiorns, R. G. Jones, R. J. M. Nolte, *Macromolecules* **2000**, *33*, 8289–8294.
[12] G. W. M. Vandermeulen, K. T. Kim, Z. Wang, I. Manners, *Biomacromolecules* **2006**, *7*, 1005–1010.
[13] H. D. Maynard, S. Y. Okada, R. H. Grubbs, *J. Am. Chem. Soc.* **2001**, *123*, 1275–1279.
[14] N. B. Holland, Y. Qiu, M. Ruegsegger, R. E. Marchant, *Nature* **1998**, *392*, 799–801.
[15] S. C. G. Biagini, A. L. Parry, *J. Polym. Sci. Part A* **2007**, *45*, 3178–3190.
[16] a) P. M. Frederik, N. A. J. M. Sommerdijk, *Curr. Opin. Colloid Interface Sci.* **2005**, *10*, 245; b) H. Cui, T. K. Hodgdon, E. W. Kaler, L. Abezgauz, D. Danino, M. Lubovsky, Y. Talmon, D. J. Pochan, *Soft Matter* **2007**, *3*, 945–955.
[17] a) S. Nickell, C. Kofler, A. P. Leis, W. Baumeister, *Nat. Rev. Mol. Cell Biol.* **2006**, *7*, 225–230; b) P. A. Midgley, P. E. P. W. Ward, A. B. Hungria, J. M. Thomas, *Chem. Soc. Rev.* **2007**, *36*, 1477–1494.
[18] a) M. R. J. Vos, P. H. H. Bomans, F. de Haas, P. M. Frederik, J. A. Jansen, R. J. M. Nolte N. A. J. M. Sommerdijk, *J. Am. Chem. Soc.* **2007**, *129*, 11894; b) T. M. Hermans, M. A.C Broeren, N. Gomopoulos, A. F. Smeijers, B. Mezari, E. N. M. van Leeuwen, M. R. J. Vos, P. C. M. M. Magusin, P. A. J. Hilbers, M. H. P. van Genderen, N. A. J. M. Sommerdijk, G. Fytas, E. W. Meijer, *J. Am. Chem. Soc.* **2007**, *129*, 15631.
[19] a) S. Han, M. Hagiwara, T. Ishizone, *Macromolecules* **2003**, *36*, 8312–8319; b) J. F. Lutz, A Hoth, *Macromolecules* **2006**, *39*, 893–896.
[20] a) J. Godward, F. Heatley, C. Price, *J. Chem. Soc. Faraday Trans.* **1993**, *89*, 3471–3475; b) F. Cau, S. Lacelle, *Macromolecules* **1996**, *29*, 170–178; c) J. Kříž , B. Masař, H. Pospíšil, J. PleŠtil, Z. Tuzar, M. A. Kiselev, *Macromolecules* **1996**, *29*, 7853–7858.
[21] The presence of both *cis* and *trans* double bonds (ratio 15:85) may be of some importance to the folding properties of the PN back bone, but no further evidence to support this suggestion is available at the moment.
[22] a) S. A. Safran, *Surf. Sci.* **2002**, *500* 127–146; b) S. Jain, F. S. Bates, *Macromolecules* **2004**, *37*, 1511–1523.
[23] Objects with similar appearance (in projection) have been observed by Eisenberg and co-workers upon addition of NaCl to vesicles of polystyrene–polyacrylic acid block copolymers; however, detailed TEM investigations of these structures under different tilt angles revealed that these intermediates were dissimilar to the structures observed in the present study: K. Yu, C. Bartels, A. Eisenberg, *Langmuir* **1999**, *15*, 7157–7167.
[24] J. G. E. M. Fraaije, G. J. A. Sevink, *Macromolecules* **2003**, *36*, 7891.
[25] Ref. [24] also predicted the formation of globules of closely associated of spherical micelles. These aggregates strongly resemble the clusters of micelles observed for PNOEG–PNGGG. However, because of the absence of detailed 3D morphological data, we cannot further confirm the structural resemblance between the two structures.

